ISIJ International, Vol. 38 (1998), No. 6, pp. 567–571

Recrystallization–Transformation Combined Reactions during Annealing of a Cold Rolled Ferritic–Austenitic Duplex Stainless Steel

Wolfgang REICK, Michael POHL[1] and Angelo Fernando PADILHA[2]

Department of Mechanical Engineering, University of São Paulo, 05508-900, São Paulo, Brazil.
1) Institute for Materials, Faculty of Mechanical Engineering, Ruhr-University, 44780 Bochum, Germany.
2) Department of Metallurgical and Materials Engineering, University of São Paulo, 05508-900, São Paulo, Brazil.
E-mail: padilha@usp.br

(Received on August 8, 1997; accepted in final form on February 5, 1998)

Solid state reactions taking place during annealing of 20% cold rolled ferrite–austenite duplex stainless steel (DIN W.-Nr: 1.4462) have been studied by means of several complementary techniques: optical, scanning and transmission electron microscopy, X-ray diffraction analysis, microhardness and ultramicrohardness measurements and magnetic phase detection (ferritoscope). It has been found that after cold rolling austenite exhibited more strain hardening and a higher driving force for recrystallization than ferrite. Extensive recovery took place in ferrite during annealing, while the deformation substructure of austenite remained nearly unrecovered until beginning of recrystallization. The recrystallization kinetics in ferrite was faster than in austenite. Recrystallization in austenite occurred in a more discontinuous manner than in ferrite. The eutectoid transformation of ferrite to sigma phase plus austenite slowed down recrystallization kinetics of both ferrite and austenite phases. A scheme is presented for sigma phase formation during recrystallization annealing.

KEY WORDS: duplex stainless steels; recovery; recrystallization; sigma phase; TTT diagrams.

1. Introduction

Metallic materials can be classified from the point of view of recrystallization phenomena in four groups: (a) pure metals; (b) single phase alloys, usually solid solutions; (c) alloys bearing a dispersion of particles and (d) duplex alloys. The alloys of type (c) very often contain less than 10% in volume of particles. For this type of alloys the recrystallization of the matrix phase is studied; the matrix is usually more ductile, and the precipitates are thought as plastically non-deformable. In the case of the alloys of type (d), with a higher quantity of a second phase, it is usually considered that the two phases deform differently and recrystallize according to distinct kinetics. Among the four types of materials above mentioned, the plastic deformation and the recrystallization of the alloys of type (d) is the least investigated.[1–3]

Duplex stainless steels have been used for several decades due to their unique mechanical and corrosion properties. These steels were introduced into the market during the thirties,[4–6] and there has been an accentuated development and rapid spreading of their use mainly during the last 15 years.[7–10] Today, duplex stainless steels are in competition with single phase austenitic and ferritic steel grades.[11]

Duplex ferritic–austenitic stainless steels contain a mixture of ferrite and austenite grains. A completely ferritic microstructure forms during solidification. Partial transformation to austenite occurs during cooling to produce precipitates of austenite in a ferrite matrix. During hot rolling and annealing, the microstructure remains within the two-phase field of the Fe–Cr–Ni phase diagram, and a microstructure forms with alternating ferrite and austenite lamellas.[12] Duplex stainless steels are processed by hot rolling or forging and cold rolling followed by suitable recrystallization annealing and quenching to equalize the proportion of the two phases.

Duplex stainless steels are interesting materials with respect to their recrystallization behaviour, due to the dissimilar characteristics of the constituents of their microstructure, ferrite and austenite. The bcc ferrite phase has numerous slip systems and a higher stacking fault energy, whereas the fcc austenite phase shows less slip systems than ferrite and a very low stacking fault energy.[13] The strain hardening and the driving force for recrystallization of austenite are actually higher than those of ferrite. Moreover, recrystallization is a diffusion activated phenomenon, and the diffusion is much faster in ferrite than in austenite. Besides, several precipitation reactions can occur in the recrystallization temperature range.[14] The most important is the precipitation of sigma phase. Formation of sigma phase frequently occurs by an eutectoid transformation from ferrite to sigma plus austenite at temperatures between 600 and 1 000°C. Sigma phase can reach high volume fractions and causes a very strong change in mechanical properties of the steels.[14–16]

The aim of this work is to give a contribution to the

understanding of the kinetics of recovery, recrystallization and formation of sigma phase and of the interactions between these combined reactions in duplex stainless steels.

2. Experimental Procedure

The material studied in this work was a commercial duplex stainless steel, DIN W.-Nr. 1.4462, the standard type duplex alloy most widely used. The initial sheet thickness was $d_0 = 1.45$ mm, and its chemical composition was 22.51% Cr; 5.6% Ni; 3.03% Mo; 0.6% Si; 1.64% Mn; 0.134% N and 0.03% C.

All samples were initially solution heat treated at 1 050°C - 30 min - WQ and subsequently cold rolled to a thickness reduction up to 20%. The cold rolled samples were annealed for periods ranging from 3 sec to 100 h between 600 and 1 000°C.

The microstructures were analyzed by several complementary techniques. They were examined by optical microscopy after color etching in Beraha I or II solutions[17] and by scanning electron microscopy (SEM) after etching in V2A-etchant.[18] Chemical analysis of the phases was carried out using an energy dispersive X-ray detector (Tracor Northern TN 2000) located in a SEM (Jeol JSM 840). Thin-foil electron microscopy (TEM) was carried out using a Philips CM20 microscope at 200 kV. Measurements of dislocation densities by X-ray diffraction analysis using a diffractometer and following a procedure proposed by Oettel[19] were carried out to compare the stored energy resulting from cold work within the two phases of the duplex steel. A Debye–Scherrer camera and a stationary flat specimen[2] were used to find out the onset of recrystallization nucleation. The kinetics of sigma phase precipitation within the duplex steel could be determined by magnetic measurements. To compare the work hardening and the softening behaviour during annealing of the ferrite and austenite phases, microhardness and ultramicrohardness were measured.

3. Results and Discussion

The results of this work will be presented and discussed in the following sequence: microstructure characterization before recrystallization annealing, and solid state reactions occurring during heat treatment after cold working.

3.1. Microstructures before Recrystallization Annealing

Table 1 shows volume fractions and mean grain diameters of ferrite and austenite in the solution heat treated condition. Grain sizes of both phases are very small, because the presence of each phase hinders grain growth of the other phase. The mean ferrite grain size is slightly higher than the austenite grain size, because of the higher mobility of atoms (diffusion) within the bcc lattice.

Table 2 shows the chemical compositions of ferrite and austenite. The values obtained by microanalytical methods and by gas chromatography are within reasonable agreement. As expected, there are higher concentrations of Cr and Mo within the ferrite phase and of Ni and N within the austenite phase.

Table 1. Volume fraction and average grain diameter of austenite and ferrite.

Phase	Austenite	Ferrite
Volume fraction in %	40	60
Average grain diameter in μm	6.3	10.8

Table 2. Chemical analysis of the main elements in ferrite and austenite (mass contents in %).

Element	Fe*	Cr*	Ni*	Mo*	N
Bulk analysis	68.15	23.38	5.30	3.17	0.14**
Austenite analysis	69.64	21.04	7.08	2.24	0.22***
Ferrite analysis	67.43	24.70	4.32	3.56	0.10***

* Energy dispersive X-ray spectroscopy (EDS).
** Gas chromatography.
*** Wavelength dispersive X-ray spectroscopy (WDS).

Table 3. Hardness and dislocation densities after solution annealing and 20% thickness reduction by cold rolling.

	Hardness* after solution annealing	Hardness* after 20% cold rolling	Dislocation density after solution annealing [1/cm²]	Dislocation density after 20% cold rolling [1/cm²]
Duplex composite	248 HV10	352 HV 10	—	—
Austenite	285 HV 0.0025	434 HV 0.0025	1.30×10^{10}	5.77×10^{11}
Ferrite	272 HV 0.0025	358 HV 0.0025	1.57×10^{9}	2.32×10^{11}

* HV 10: measurements using a Vickers hardness tester with 10 kg load; HV 0.0025: measurements using a Vickers ultramicrohardness tester with 0.0025 kg load.

Both phases presented relative high dislocation densities after solution annealing (**Table 3**). Probably most of these dislocations were introduced during cooling from the annealing temperature. In duplex stainless steels the constituent phases austenite and ferrite have different coefficients of thermal expansion. As temperature changes, a stress state develops and the yield strength of the phases can be exceeded.[20]

By cold rolling, up to 20% thickness reduction, hardness and dislocation densities of the two phases were highly increased, as shown in Table 3.

Both hardness and dislocation density measurements showed that austenite exhibited more strain hardening and consequently a higher driving force for recrystallization than ferrite. For instance, ferrite hardness increased by 32% and austenite hardness by 52% after 20% thickness reduction.

Transmission electron microscopy observation showed dislocation cell formation in ferrite and a much more uniform dislocation distribution with high incidence of stacking faults in austenite. The strain hardening be-

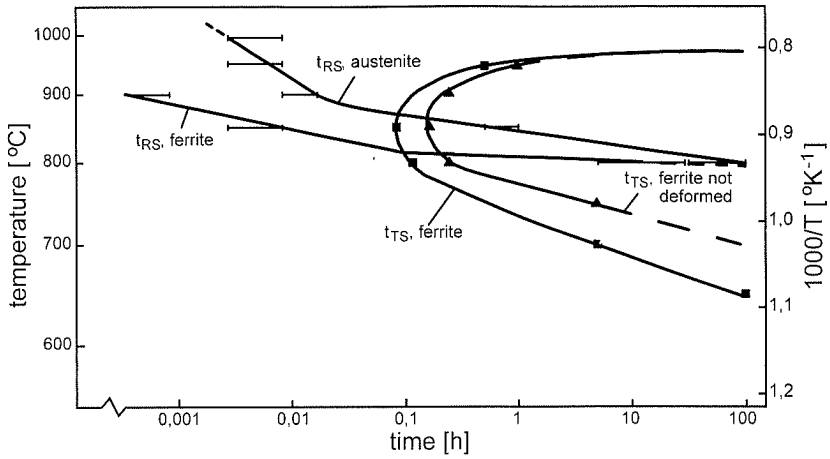

Fig. 1. Time–temperature–transformation diagram after solution annealing (curve ▲) and after 20% thickness reduction by cold rolling (all other curves). RS = recrystallization start; TS = start of the eutectoid transformation from ferrite to sigma plus austenite.

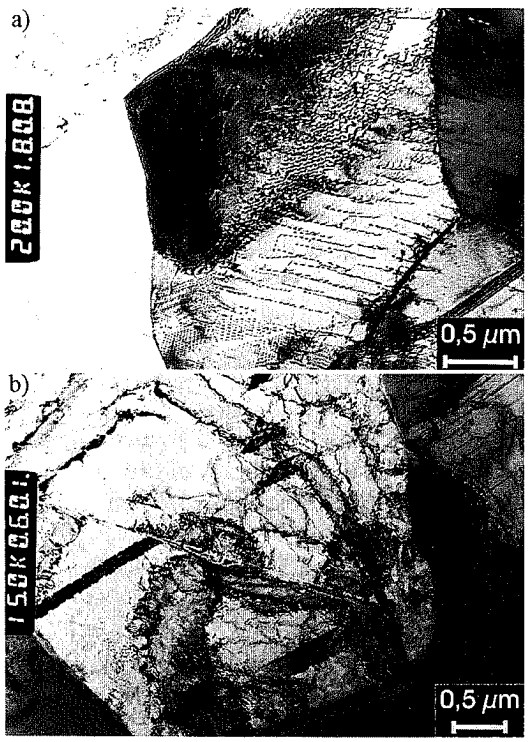

Fig. 2. TEM bright field images (rolling plane) of a duplex stainless steel after 20% deformation, annealing time 1 min at 950°C. a) well recovered dislocation substructure in ferrite. b) nearly unchanged deformation substructure of the austenite phase.

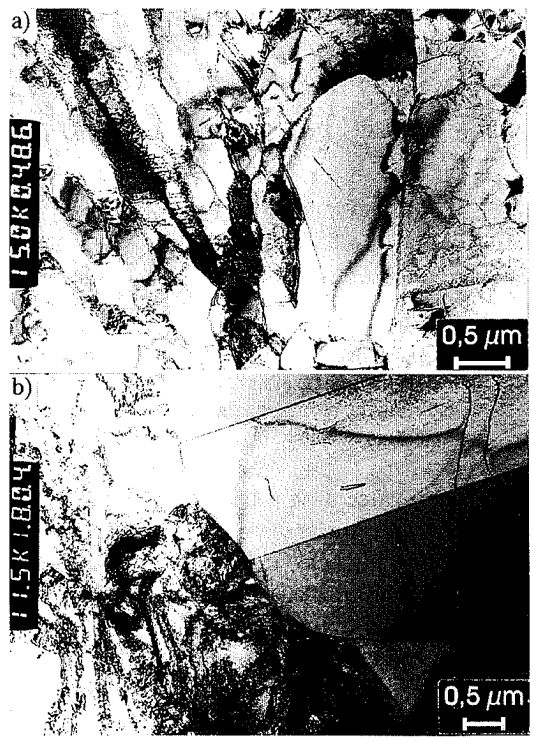

Fig. 3. TEM bright field images (rolling plane) of a duplex stainless steel after 20% deformation. a) formation of recrystallization nuclei resulting from subgrain growth after annealing time 10 min at 850°C. b) discontinuous recrystallization in austenite nearby ferrite/austenite interface after 1 min at 950°C.

haviour of this steel is discussed in more details elsewhere.[13)]

3.2. Solid State Reactions during Recrystallization Annealing

During heat treatment of the cold rolled duplex stainless steel, at least five solid state reactions occurred: recovery and recrystallization of austenite, recovery and recrystallization of ferrite and eutectoid transformation of ferrite to sigma phase plus austenite. With the aid of the time–temperature–transformation diagram in **Fig. 1** it is possible to separate the different solid state reactions occurring within the two phases as a function of time and temperature.

For a given temperature, the time periods of predominantly recovery are always on the left side of the recrystallization start curves (t_{RS}). Extensive recovery processes took place in ferrite on annealing, while the deformation substructure of the austenite phase remained nearly unchanged until the beginning of recrystallization. This behaviour is exemplified in the micrographs of **Fig. 2.** There are at least three reasons for this: higher dislocation mobility in ferrite than in austenite (the fcc phase shows less slip systems than ferrite and very low stacking fault energy[13)]), more favorable dislocation arrangements in ferrite (dislocation cell substructure) and

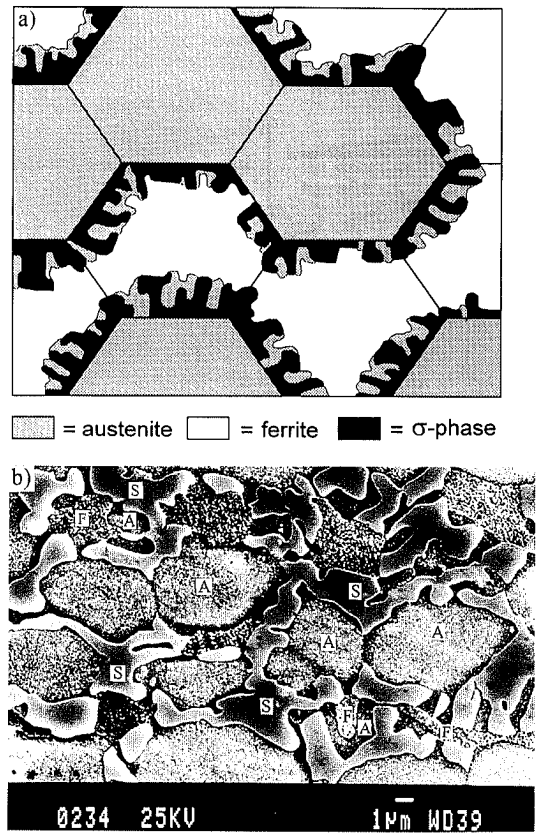

Fig. 4. Sigma phase formation during the eutectoid transformation ferrite→sigma phase + austenite; a) scheme for sigma phase nucleation on ferrite/austenite interfaces and growth into ferrite; b) SEM micrography (secondary electrons image) after 850°C/30 min heat treatment illustrating the proposed scheme (F = ferrite; S = sigma phase; A = austenite).

higher diffusion rates within the bcc lattice.

Recrystallization nuclei were formed in ferrite by subgrain growth (see **Fig. 3a)**) in a well recovered substructure, whereas recrystallization in austenite occurred in a more discontinuous manner (**Fig. 3b)**), preferentially at ferrite/austenite interfaces. For all heat treatments, the onset of ferrite recrystallization took place at lower temperatures and at shorter times than that of austenite recrystallization (see Fig. 1), despite of the higher driving force for recrystallization of austenite. For both recovery and recrystallization, the lower stored energy during cold working within the ferrite phase was overcompensated by the higher diffusivity and dislocation mobility in the bcc lattice, resulting in an overall recrystallization process faster in ferrite.

The sigma phase formation occurred predominately by an eutectoid transformation from ferrite to sigma plus austenite. Sigma precipitates were observed to nucleate at the ferrite/austenite interfaces and then grow into the ferrite grains. Two solid state reactions are responsible for the formation of austenite in duplex stainless steels: the direct decomposition of ferrite into austenite at about 1 250°C and the above mentioned eutectoid reaction $\alpha \rightarrow \sigma + \gamma$. In this second reaction mode the sigma formation leads to regions depleted in ferrite stabilizing elements such as chromium and molybdenum and consequently to austenite formation. Nucleation of sigma phase along ferrite/ferrite grain boundaries and a direct reaction $\alpha \rightarrow \sigma$ may also occur. **Figure 4a)** presents a scheme for nucleation and growth of the sigma phase, which can be observed in the micrograph of **Fig. 4b)**. This micrograph shows that the eutectoid phases morphology are poorly lamellar.

Heat treatments up to 100 h were insufficient to cause sigma phase precipitation in austenite. On the other hand, cold work accelerated sigma occurrence in ferrite. For instance, at about 850°C the sigma formation started after only some minutes.

Furthermore, the recrystallization start curves of ferrite and austenite in Fig. 1 show a sharp bend near the beginning of sigma phase formation. The interaction between precipitation and recrystallization of supersaturated single phase solid solutions was extensively discussed and schematized in the classical work of Hornbogen and Köster.[21] In the present work (duplex alloy), the sigma formation within ferrite slowed down the recrystallization kinetics not only of the ferrite, but also of the austenite phase. An explanation for this behaviour is the preferential sigma formation at ferrite/austenite interfaces, decreasing the number of possible nucleation sites for austenite recrystallization. The formation of recrystallization nuclei is difficult in the austenite (fcc structure with low stacking fault energy) because the dissociated dislocations cannot rearrange easily. Therefore the ferrite/austenite interfaces act as preferred sites for a discontinuous recrystallization reaction.

The analysis of the curves in Fig. 1 suggests that the sharp bend in the austenite recrystallization curve occurred before the onset of sigma formation. This fact can be explained by the inaccuracy of the used measuring method employed (ferritoscope) to detect the onset of sigma formation.

4. Conclusions

The experiments performed in this work, the analysis and discussion of the results lead to the following conclusions:

(1) After cold work, the austenite phase of the duplex stainless steel studied exhibited more strain hardening and consequently a higher driving force for recrystallization than the ferrite phase. Microstructure investigation showed dislocation cell formation within ferrite and a much more uniform dislocation distribution with high incidence of stacking faults in austenite.

(2) Extensive recovery processes took place in ferrite on annealing, while the deformation substructure of the austenite phase remained nearly unchanged until beginning of recrystallization.

(3) Recrystallization nuclei were formed in ferrite by subgrain growth in a well recovered substructure, whereas recrystallization in austenite occurred in a more discontinuous manner, preferentially at ferrite/austenite interfaces.

(4) The overall recrystallization kinetics was faster in ferrite than in austenite, despite of the higher driving force for recrystallization in austenite.

(5) The sigma formation within ferrite slowed down recrystallization kinetics not only of the ferrite, but also of the austenite phase.

Acknowledgments

The authors are grateful to Prof. Dr.-Ing. Erhard Hornbogen (Ruhr-University, Bochum, Germany) for helpful discussions and suggestions. Dr.-Ing. Paul Schwaab is thanked profusely for his support during the TEM investigations. Thanks are also due to Prof. Dr. Paulo Sérgio Carvalho Pereira da Silva (University of São Paulo, Brazil) for going through the manuscript meticulously.

REFERENCES

1) K. Mäder: Dr.-Ing. Thesis, Ruhr-University, Bochum, Germany, (1973).
2) W. Reick: Dr.-Ing. Thesis, Ruhr-University, Bochum, Gemany, (1993).
3) M. Blicharski: *Met. Sci.*, **18** (1984), 99.
4) E. C. Bain and W. E. Griffiths: *Trans. AIME*, **75** (1927), 166.
5) The AVESTA Duplex History; Poster at the Conf. on Duplex Stainless Steels, Beaune, France, (1991).
6) J. Holtzer: *Brevets Français*, 803-361, (1935), 49.211, (1937) and 866-685, (1940).
7) J. Olsson and S. Nordin: Int. Conf. on Duplex Stainless Steels, Nederlands Instituut voor Lastechniek, Den Haag, (1986), 219.
8) W. Reick: M. Sc. Thesis, Ruhr-University, Bochum, Germany, (1989).
9) J. Charles: Duplex Stainless Steels '91, Conf. Proc., ed. by J. Charles and S. Bernhardsson, Vol. 1, les éditions de physique, Les Ulis, France, (1991), 3.
10) W. Reick, M. Pohl and A. F. Padilha: *Metalurgia Int.*, ABM, São Paulo, Brazil, **3** (1990), 46.
11) W. Reick, M. Pohl and A. F. Padilha: *Metalurgia Mater.*, ABM, São Paulo, Brazil, **48** (1992), 551.
12) M. Pohl and A. F. Padilha: *Nickel*, **3** (1988), 7.
13) W. Reick, M. Pohl and A. F. Padilha: *Steel Res.*, **67** (1996), 253.
14) P. Schwaab: *Sonderbände Prakt. Metallogr.*, **14** (1983), 435.
15) L.-A. Norström, S. Pettersson and S. Nordin: *Z. Werkstofftech.*, **12** (1981), 229.
16) T. Chandra and R. Kuchmayr: *J. Mater. Sci.*, **23** (1988), 723.
17) E. Weck and E. Leistner: Metallographische Anleitung zum Farbätzen nach dem Tauchverfahren, Teil II, Deutscher Verlag für Schweisstechnik, München, (1983).
18) G. Petzow: Metallographisches Ätzen, Gebrüder Bornträger, Berlin, (1984).
19) H. Oettel and G. Heide: Lehrbrief für das Hochschulfernstudium, Zentralstelle für Hoch- und Fachschulwesen (Hrsg.), Bergakademie Freiberg, Germany, (1978), 32.
20) T. Siegmund, E. Werner and F. D. Fischer: *Mater. Sci. Eng.*, **A169** (1993), 125.
21) E. Hornbogen and U. Köster: Recrystallization of Metallic Materials., ed. by F. Haessner, Riederer-Verlag, Stuttgart, Germany, (1978), 159.